PHYSICAL REVIEW B VOLUME 52, NUMBER 15 15 OCTOBER 1995-I

ARTICLES

Transport velocity in two-dimensional random media

K. Busch
Institut für Theorie der Kondensierten Materie, Universität Karlsruhe, 76128 Karlsruhe, Germany

C. M. Soukoulis
Ames Laboratory and Department of Physics and Astronomy, Iowa State University, Ames, Iowa 50011

E. N. Economou
Research Center of Crete, Foundation for Research and Technology–Hellas (FORTH) and Department of Physics, University of Crete, P.O. Box 1527, 71110 Heraklion, Crete, Greece
(Received 6 June 1995)

We study the transport properties of a two-dimensional randomly disordered dielectric medium. The medium consists of infinitely long dielectric cylinders with a real dielectric constant ϵ_a, embedded in a different dielectric medium with $\epsilon_b = 1$. The transport velocity is calculated within the low-density approximation of the Bethe-Salpeter equation and within the coated extension of the well-known coherent-potential approximation for a random arrangement of dielectric cylinders. Results for the long-wavelength effective dielectric constant, phase velocity, and transport velocity are presented for both the s and p polarization of electromagnetic waves. In addition, it is found that localization is achieved more easily for the s than for the p polarization.

I. INTRODUCTION

Recently, there has been a growing interest in the propagation of electromagnetic (EM) waves in random media,[1] and in periodic (both in two and three dimensions) structures, the so-called photonic band structures.[2] Although strong localization of classical waves has yet to be observed experimentally, weak localization or enhanced coherent backscattering has been detected in light-scattering experiments.[1] It was recently reported[3] that a very small energy transport velocity v_E enters the diffusion constant $D = v_E \ell_t/3$. The extremely small experimental values of D were caused by the small values of v_E and not by the small values of the transport mean free path ℓ_t, which signifies strong localization. It is by now well understood[3–5] that to "lowest order in density" of the dielectric scatterers, the strong decrease in the transport velocity is due to the single scatterer Mie resonances. Near resonances, a lot of energy is temporarily stored inside the dielectric scatterer or equivalently the wave spends a lot of time (dwell time) inside the dielectric scatterer. Experimental results[6] for alumina spheres have shown that as the volume fraction f of the scatterers increases towards close packing, there is no structure in D and therefore v_E, versus frequency. The low-density theory of van Albada *et al.*[3] gives strong structure in v_E, even for high f, in disagreement with the experiment. An extension of the well-known coherent potential approximation (CPA) was developed[7] recently and obtained a CPA phase velocity for high f, which is qualitatively consistent with experiment, in not showing any structure as a function of frequency. Unfortunately, the coated CPA for low f gives a CPA phase velocity that reduces to the regular phase velocity and can, therefore, be higher than the velocity of light near Mie resonances. Thus, for small f, the theory of van Albada *et al.*[3] seems to give the correct transport velocity v_E, while for large f, it is the coated-CPA approach,[7,8] which seems to give transport velocities consistent with experiment. Soukoulis, Datta, and Economou[7] have combined these two approaches and have calculated the transport velocity for general f, with qualitative agreement with experiment, in the following way. The coated-CPA is used to calculate a frequency-dependent effective dielectric function $\bar{\epsilon}$; then the energy velocity expression of van Albada *et al.*[3] was used to calculate v_E with this $\bar{\epsilon}$ as the outside medium. However, this is not a very clean theoretical approach, since it combines the low-density theory of van Albada *et al.*[3] with the coated-CPA approach. Recently, Busch and Soukoulis[9] presented a new approach for calculating the transport properties of random media. It is based on the principle that the wave energy density should be uniform when averaged over length scales larger than the size of the scatterers. It has been successfully applied to both scalar and vector classical wave calculations, and works for all frequencies and scatterer concentrations.

In this paper, we present results for the transport properties of two-dimensional (2D) random dielectric cylin-

0163-1829/95/52(15)/10834(7)/$06.00 ©1995 The American Physical Society

ders. First, we give a microscopic derivation of the energy transport velocity for both s and p polarization. The transport theory developed by van Albada *et al.*[3] for 3D is extended to the 2D case. The long-wavelength limit of the effective dielectric constant is calculated and compared with the coated-CPA results, as well as the predictions of the low-density approximation of the Bethe-Salpeter equation. The dimensionless localization parameter $k\ell$ where k is the wave vector and ℓ is the mean free path, is calculated within the coated-CPA approach. Localization is achieved more easily for the s than for the p polarization.

For EM waves propagating in the x, y plane, the s- (E field parallel to the z axis) and p- (E field perpendicular to the z axis) polarized waves can be described by two decoupled wave equations.¶5itebib10 The equation for the s-polarized wave is

$$\nabla^2 E + \frac{\omega^2}{c^2}\,\epsilon\, E = 0 \quad , \tag{1}$$

where $E = E_z$, $\epsilon = \epsilon(\mathbf{r})$ is the dielectric constant, ω is the frequency, and c is the speed of light in vacuum. Equation (1) is identical to the scalar wave equation. The equation for the p-polarized wave has the form:

$$\nabla\left(\frac{\nabla H}{\epsilon}\right) + \frac{\omega^2}{c^2}\,H = 0 \quad , \tag{2}$$

where $H = H_z$. Using plane-wave expansion methods, one can solve the previous two equations for a periodic lattice and, therefore, find the band structure.[10–14] The 2D structures were made of parallel dielectric rods in air or cylindrical air holes in a dielectric material. The objective was to find the geometry that would yield the largest gap for the smallest index contrast. Finding structures that have overlapping band gaps for both polarizations is possible, but such structures are rare. The triangular lattice of air cylinders and the honeycomb lattice of dielectric cylinders are the only ones[12,13] known until now. It is now well understood[13–15] that another parameter for obtaining a complete band gap is the connectivity of the dielectric components of the structure. In the case of s-polarized waves (scalar waves) high dielectric cylinders in a low dielectric medium are more effective in giving a photonic band gap. On the other hand, for p-polarized waves (vector waves) low dielectric cylinders in a high dielectric medium are more effective in giving a photonic band gap. Experimental investigations[16,17] of the 2D photonic band gaps with or without defects have been mostly done at microwave frequencies. Little[17] or no work has been done for the transport properties such as the transport velocity, mean free path, and the localization parameter $k\ell$ of EM waves propagating in 2D disordered dielectric systems.

II. ENERGY TRANSPORT VELOCITY IN 2D AND 3D

In this section we will give a microscopic derivation of the transport velocity for EM waves propagating in random 2D and 3D random media. We will follow closely the formalism of van Tiggelen and Lagendijk[3] developed for the 3D case, in the low-density approximation. We will not repeat all the steps here, but we will present the final result, which is applicable to both two and three dimensions. By correctly handling the Ward identities, the Amsterdam group[3] reported that in the low-density limit the diffusion coefficient $D = v_E \ell_t/3$, where the energy transport velocity v_E is given by

$$v_E = \frac{c^2}{v_p(1+n\delta)} \quad . \tag{3}$$

The quantity δ is given by

$$\delta = \int d^3r\, |\psi_k(r)|^2\, [\epsilon(r) - 1] \quad , \tag{4}$$

where n is the number density of scatterers and $\psi_k^+(r)$ is the one-scatterer eigenfunction with incident wave vector k for a single dielectric scatterer. A more elegant, and most convenient for numerical purposes, representation of δ for scalar and vector waves, was given by van Tiggelen and Lagendijk[3] for 3D. There δ and, therefore, v_E were written with respect to the van de Hulst scattering coefficients of the scalar or vector dielectric sphere. We have obtained a general expression for δ, which is correct for both the 2D and 3D cases. The quantity δ is given by

$$\delta = -\mathrm{Re}\left[\frac{\partial}{\partial p^2}\, t^{(d)}_{\mathbf{pp}}(p)\right] + \int d\Omega_d\, \frac{d\sigma^{(d)}}{d\Omega}\, \frac{\partial \phi^{(d)}_{\mathbf{pp}'}(p)}{\partial p} \quad , \tag{5}$$

where the differential cross section is defined as

$$\frac{d\sigma^{(d)}}{d\Omega} = p^{1-d}\, |\tilde{t}^{(d)}_{\mathbf{pp}'}|^2 / 4(2\pi)^{d-1} \quad , \tag{6a}$$

and

$$t^{(d)}_{\mathbf{pp}'} = p^{2-d}\, \tilde{t}^{(d)}_{\mathbf{pp}'} \quad . \tag{6b}$$

Here $\phi^{(d)}_{\mathbf{pp}'}$ denotes the phase of the d-dimensional t-matrix element according to $t_{\mathbf{pp}'} \equiv |t_{\mathbf{pp}'}| \exp(i\phi_{\mathbf{pp}'})$, Ω_d is the surface of the unit sphere in d dimensions, and $\omega = pc$. The t matrix for the 3D case is given[18,19] by

$$\tilde{t}^{(3)}_{\mathbf{pp}'}(\omega = pc) = -4\pi i \begin{pmatrix} S_2^*(\theta)\cos\phi & 0 \\ 0 & S_1^*(\theta)\sin\phi \end{pmatrix} \quad , \tag{7}$$

where

$$S_1(\theta) = \sum_{n=1}^{\infty} \frac{2n+1}{n(n+1)} \left[a_n \pi_n(\theta) + b_n \tau_n(\theta)\right], \tag{8a}$$

$$S_2(\theta) = \sum_{n=1}^{\infty} \frac{2n+1}{n(n+1)} \left[a_n \tau_n(\theta) + b_n \pi_n(\theta)\right], \tag{8b}$$

where

$$\pi_n(\theta) = \frac{P_n^1(\cos\theta)}{\sin\theta}, \tag{9a}$$

$$\tau_n(\theta) = \frac{d\,P_n^1(\cos\theta)}{d\theta}, \tag{9b}$$

here $P_n^1(\cos\theta)$ are associated Legendre polynomials. It is convenient to introduce the phase of the the van de Hulst scattering coefficients[18,19] a_n and b_n,

$$a_n = [1 - \exp(-2i\alpha_n)]/2, \tag{10a}$$

$$b_n = [1 - \exp(-2i\beta_n)]/2. \tag{10b}$$

Substituting the above expression for the t matrix in Eq. (3), and by differentiation of the first term of the right-hand side of Eq. (5) and direct integration of the second term one obtains that the quantity δ for the 3D case is given[3] by

$$\delta = -\frac{2\pi}{\omega^3}\sum_{n=1}^{\infty}(2n+1)\,\mathrm{Im}[a_n + b_n] + \frac{\pi}{\omega^2}\sum_{n=1}^{\infty}(2n+1)\left[\frac{d\alpha_n}{d\omega} + \frac{d\beta_n}{d\omega}\right]. \tag{11}$$

The t matrix for the 2D case is given[18,19] by

$$\tilde{t}_{pp'}^{(2)}(\omega = pc) = -4i\;T_j(\theta)\quad, \tag{12}$$

where

$$T_j(\theta) = c_{0j} + 2\sum_{n=1}^{\infty} c_{nj}\cos(n\theta)\quad. \tag{13}$$

The index j refers to the two polarizations of the incident EM wave.

For the s polarization ($j = 1$) we have that $c_{nj} = b_n$, while for the p polarization ($j = 2$) $c_{nj} = a_n$. The coefficient a_n for the p polarization and b_n for the s polarization are given[18,19] by

$$a_n = \frac{J_n'(y)J_n(x) - mJ_n(y)J_n'(x)}{J_n'(y)H_n(x) - mJ_n(y)H_n'(x)}, \tag{14a}$$

and

$$b_n = \frac{mJ_n'(y)J_n(x) - J_n(y)J_n'(x)}{mJ_n'(y)H_n(x) - J_n(y)H_n'(x)}, \tag{14b}$$

where the primes denote derivatives, $x = kR$, and $y = mx$. J_n and H_n are the Bessel and Hankel functions of integer order, R is the radius of the cylinders, m is the relative index of refraction of the cylinder, and k is the magnitude of the EM wave vector in free space. For the 2D case, too, one can define the corresponding phases γ_{nj} of the van de Hulst coefficients for both polarizations

$$c_{nj} = [1 - \exp(-2i\gamma_{nj})]/2\;. \tag{15}$$

Substituting the above expressions for the 2D t matrix in Eq. (5) one can easily obtain that the quantity δ_j for the 2D case is given by

$$\delta_j = \frac{2}{\omega}\left[\frac{d\gamma_{0j}}{d\omega} + 2\sum_{n=1}^{\infty}\frac{d\gamma_{nj}}{d\omega}\right]\quad, \tag{16}$$

where $j = 1$ and 2 are the s- and p-polarized cases. By determining the 2D filling ratio $f = \pi R^2 n$ one can use Eq. (1) to obtain the energy transport velocity v_E for propagation of EM waves in 2D random media. In fact, we have that

$$v_{Ej} = \frac{c^2}{v_p}\left[1 + \frac{2}{\pi}\frac{f}{x}\left(\frac{d\gamma_{0j}}{dx} + 2\sum_{n=1}^{\infty}\frac{d\gamma_{nj}}{dx}\right)\right]^{-1}\quad, \tag{17}$$

where the index j again defines the two polarizations. The phase velocity v_p can be calculated from the disorder averaged Green's function and is given by

$$v_{pj} = c\sqrt{1 - \mathrm{Re}\,\Sigma_j/p^2}\quad, \tag{18}$$

where Σ is the self-energy and in the weak scattering approximation $\Sigma_j = -2\pi n f_j(0)$. $f_j(0)$ is the forward scattering amplitude from an infinite dielectric cylinder, and is given by

$$f_j(0) = \frac{i}{2p}\left(c_{0j} + 2\sum_{n=1}^{\infty} c_{nj}\right)\quad. \tag{19}$$

We have numerically calculated the energy transport velocity v_E, given by Eq. (17) and the phase velocity v_p given by Eq. (18) for both polarizations in 2D random arrangement of dielectric cylinders. The dielectric constant of the cylinder is $\epsilon_a = 9$ and that of the background is equal to 1. In Fig. 1(a), we present the results for the phase velocity v_p and the energy transport velocity v_E for the s polarization. The filling ratio $f = 0.20$ and the dielectric constant of the cylinder is equal to 9.0. Notice that v_E is always less than v_p for all frequencies. We have chosen to present our results versus d/λ_i, which is proportional to frequency, since $\lambda_i = 2\pi c/\omega\sqrt{\epsilon_a}$ is the wavelength inside the cylinder and d is the diameter of the cylinder. We choose to present our results this way, since strong Mie resonances appear in the total scattering cross section from the isolated cylinder in the limit of $\epsilon_a/\epsilon_b \to \infty$ when $d/\lambda_i = (n+1)/2$ with $n = 0, 1, 2, 3$. Notice that both the phase velocity and the energy transport velocity give a lot of structure, especially close to the Mie resonances. This is expected because both of these quantities were calculated within a theory valid for the low concentration limit, i.e., for just one isolated scatterer. Similar results are observed for the p polarization shown in Fig. 1(b). The phase velocity can give unphysical values, i.e., v_p/c can be larger than 1, especially close to the isolated Mie resonances. The energy transport velocity v_E differs considerably from v_p and is always lower than v_p, but has a lot of spurious structure due to its calculation procedures which are based on scattering from a single isolated scatterer. As in the 3D case,[3] v_E for the 2D case can be considerably lower than v_p. It will be very interesting to perform experiments on 2D to check

the predictions obtained for v_E. In the long-wavelength limit, both v_E and v_p give the same value. For the s polarization, the long-wavelength limit of the effective dielectric constant ϵ_e is equal to

$$\epsilon_e = f\epsilon_a + (1-f)\epsilon_b \quad , \tag{20a}$$

with $\epsilon_a = 9$ and $\epsilon_b = 1$ for our case of dielectric cylinders with $\epsilon_a = 9$ in a background with $\epsilon_b = 1$. This was expected, since for the s polarized case, the wave equation is given by Eq. (1), which is identical to the scalar wave equation. The long-wavelength limit of the scalar wave equation is indeed given by Eq. (20a). The p-polarized case is described by Eq. (2), which is like a vector equation. In the low-density approximation, the long-wavelength limit of ϵ_e, is now given by

$$\epsilon_e = \epsilon_b \left(1 + 2f\frac{\epsilon_a - \epsilon_b}{\epsilon_a + \epsilon_b}\right) \quad . \tag{20b}$$

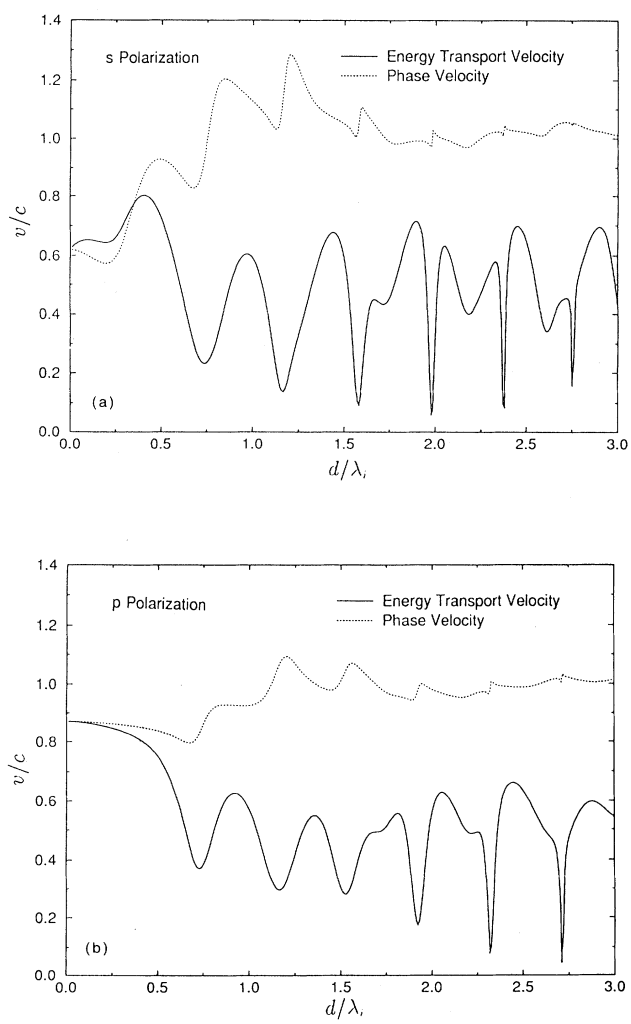

FIG. 1. The phase velocity and the energy transport velocity vs d/λ_i for $\epsilon_a = 9.0$ dielectric cylinders with filling ratio $f = 20\%$, for (a) s and (b) p polarization. d is the diameter of the sphere and $\lambda_i = 2\pi c/\omega\sqrt{\epsilon_a}$ is the wavelength inside the cylinder.

Equation (20b) can be obtained by taking the long-wavelength limit of Eq. (17). It can also be derived from the electric dipole contribution.[19] The correct long-wavelength limit of ϵ_e, which is correct not only in the low-density approximation as is Eq. (20b), but for all concentrations f, is the following expression:

$$\epsilon_e = \epsilon_b \left(1 + \frac{2f\alpha}{1 - f\alpha}\right) \quad , \tag{20c}$$

with $\alpha = (\epsilon_a - \epsilon_b)/(\epsilon_a + \epsilon_b)$. This is the Maxwell-Garnett result for the 2D case. Of course, Eq. (20c) goes to Eq. (20b) as $f \to 0$, i.e., in the low-density approximation. In Fig. 2, the Maxwell-Garnett theory results of Eq. (20c) (solid line) are shown for the case with $\epsilon_a = 9$ and $\epsilon_b = 1$, and f is the concentration of the ϵ_a dielectric cylinder. In the same figure, the long-wavelength limit for the s-polarized case [Eq. (20a)] is also presented (solid line). The circles and squares are the predictions of the coated CPA for s and p polarization, respectively. Notice that the predictions of the coated CPA, for dielectric cylinders, for the long-wavelength limit agree remarkably well with the theory of the scalar (s-polarized) and vector (p-polarized) cases.

III. COATED CPA FOR 2D RANDOM MEDIA

The CPA calculates the wave propagation characteristics of a random system by replacing it by a uniform effective one of dielectric constant ϵ_e. The effective ϵ_e is calculated by demanding that the scattering produced when the effective medium is locally replaced by configurations[7,8,20,21] of the actual system is on the average equal to zero. Therefore, the quantity ϵ_e is self-

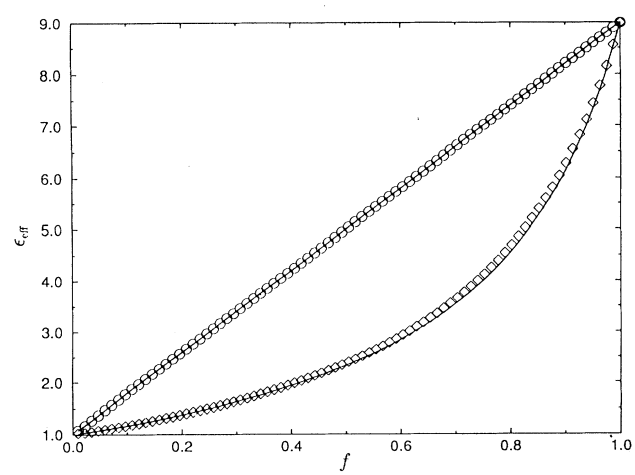

FIG. 2. The long-wavelength dielectric constant $\epsilon_{\rm eff}$ for a cylinder with dielectric constant $\epsilon_a = 9$ in a background of $\epsilon_b = 1$ as a function of the cylinder filling ratio f. The CPA results for s polarization (open circles) and p polarization (open squares) are presented. The solid lines represent the analytical scalar [Eq. (20a)] and Maxwell-Garnett [Eq. (20c)] results.

consistently determined by demanding that the average forward-scattering amplitude $f(0)$ is equal to 0. Once the complex frequency-dependent effective dielectric constant ϵ_e is determined by an effective propagation constant q is defined as

$$q = \left(\frac{\omega^2}{c^2}\epsilon_e\right)^{1/2} = k + i/2\ell \ , \tag{21}$$

where k is the wave vector and ℓ is the scattering mean free path. In the present case where each cylindrical scatterer has a finite size, the differential cross section requires an infinite number of coefficients for its complete determination, while the effective medium is characterized by only two parameters, namely, k and ℓ. Thus, the question arises as to which averaged scattering quantity should be set equal to 0. We have decided to set the so-called average forward-scattering amplitude $\langle f(0)\rangle = 0$. We have recently considered[7] as basic scattering units a coated sphere of the high dielectric material and a sphere of the host, low dielectric material. We have extended the coated-CPA formalism to treat the transport properties of a random arrangement of dielectric cylinders. Within the coated CPA, one has to satisfy the following condition: $p_1 f_1(0) + p_2 f_2(0) = 0$, where p_1 and $f_1(0)$ are the probability and the forward-scattering amplitude of a coated solid cylinder embedded in the effective medium with dielectric constant ϵ_e; p_2 and $f_2(0)$ are corresponding quantities of a host cylinder embedded in the effective medium. The forward-scattering amplitudes, as well as the total scattering cross section σ of either a coated cylinder or a host cylinder for both polarizations are given in Appendix A. To solve the equation $\langle f(0)\rangle = 0$ or equivalently $\langle\Sigma\rangle$=0, we have transformed it into an iterative equation of the form $q_{i+1} = q_i + A\langle\Sigma\rangle$, where i is the order of the iteration and A is chosen using the weak scattering limit and demanding as good a convergence as possible. For the 2D case, we have a lot of problems with the convergence, much more than the 3D case. However, after a successful convergence of q, which implies $\langle f(0)\rangle = 0$ or $\langle\Sigma\rangle = 0$, the mean free path $\ell = 0.5/\mathrm{Im}(q)$, the renormalization wave vector $k = \mathrm{Re}(q)$, the dimensionless localization parameter $k\ell$, and the effective CPA phase velocity $v_{\mathrm{CPA}} = \omega/k$ are determined. The only free parameter in the coated-CPA approach[7] is the quantity z, which was fixed to be equal to $z = 3$ in the 2D case. This choice gives an excellent agreement between the coated-CPA results and the Maxwell-Garnett theory for the long-wavelength effective dielectric constant ϵ_e for all values of f. This is clearly shown in Fig. 2, where we plot ϵ_e vs f. The circles and squares give our coated-CPA results for s and p polarization, respectively, and agree extremely well with the analytical results (solid lines).

To further check the coated CPA, we have calculated the CPA phase velocity defined as ω/k [see Eq. (21)]. In Fig. 3(a), we present the frequency dependence of the CPA phase velocity for two filling ratios f of alumina rods, with $\epsilon_a = 9$, for the s polarization. Notice there is structure in the CPA phase velocity v_{CPA} for $f = 0.20$, but not as much as the energy transport velocity in Fig. 1(a). The CPA phase velocity for $f = 0.60$ has little or no structure as d/λ_i varies and v_{CPA} stays below c. In Fig. 3(b), we present the frequency dependence of v_{CPA} for $f = 0.20$ and 0.60 of the alumina rods with $\epsilon_a = 9$ for the p polarization. In this case, notice that there is a strong structure in the v_{CPA} for $f = 0.20$ and takes values higher than c, as the phase velocity in the Fig. 1(b). However, in the p-polarized case too, as f increases ($f = 0.60$) little or no structure is shown as d/λ_i varies. It is extremely important to experimentally measure the transport velocity of EM waves propagating in an arrangement of random dielectric cylinders, for both polarizations. We have also calculated the energy transport velocity derived from Eq. (17) for $f = 0.60$ for both polarizations and we find that, as in the 3D case,[7] v_E shows strong structure as d/λ_i varies. It would be, therefore, interesting to have additional careful experiments of the frequency dependence of the transport velocity for the 60% case of alumina rods to see if there is any structure in the transport velocity.

As a final check of our 2D coated CPA, we calculated

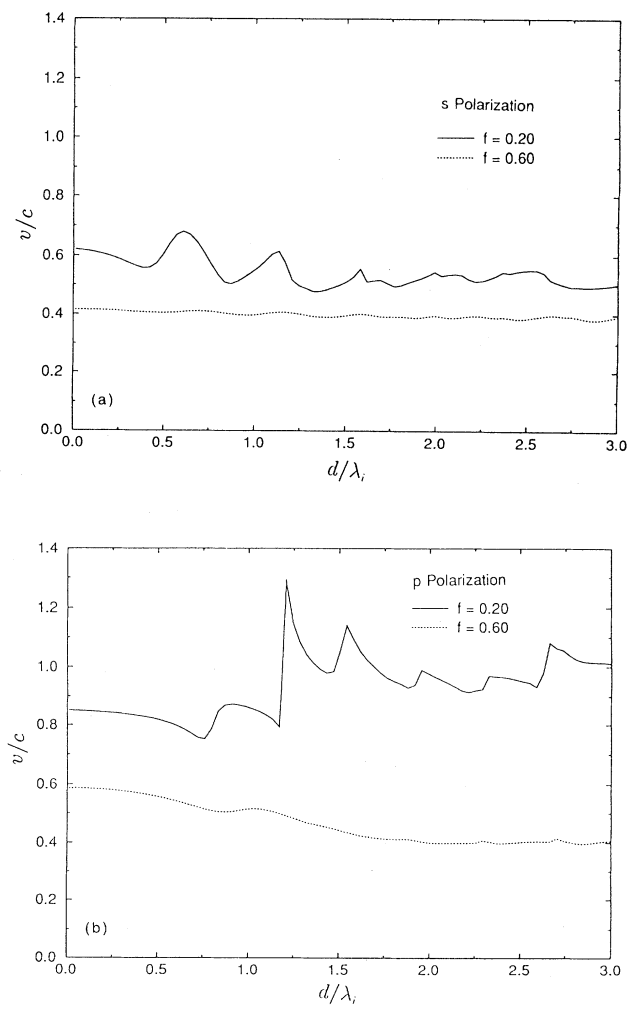

FIG. 3. The effective phase velocity, calculated within the coated CPA vs d/λ_i for alumina cylinders with dielectric constant $\epsilon_a = 9$ for different values of filling ratios for (a) s and (b) p polarization.

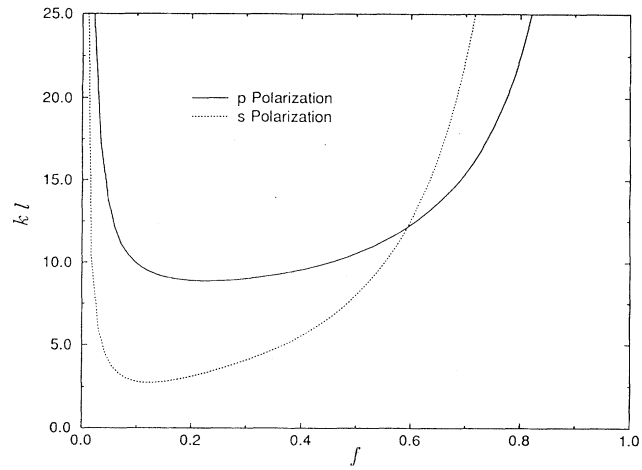

FIG. 4. The localization parameter $k\ell$ vs the filling ratio f for alumina cylinders with $\epsilon_a = 9$ for frequency $d/\lambda_i = 0.7$ for both s and p polarization.

the localization parameter $k\ell$ vs f, for low frequencies, i.e., when $d/\lambda_i = 0.7$. If $k\ell$ is large the states are extended or weakly localized, i.e., the localization length might be extremely large. However, as $k\ell$ decreases the states become more localized. In Fig. 4, we present the results for $k\ell$ vs f for $d/\lambda_i = 0.7$ and $\epsilon_a = 9$ and $\epsilon_b = 1$. Notice that for the s-polarized case (dotted line) $k\ell$ has a minimum value of $k\ell \simeq 3$ when $f \simeq 0.10$. For the p-polarized case (solid line) $k\ell$ is always larger than the s-polarized case and has a broad minimum value of $k\ell \simeq 10$ when $f \simeq 0.30$. These results clearly suggest that localization for the s-polarization case is inherently easier than the p polarization. These results are in qualitative agreement[15] with recent numerical results of the propagation of EM waves in 2D disordered systems, which clearly demonstrated that localization is achieved more easily for the s-polarized case than the p-polarized case.

IV. CONCLUSIONS

In this paper, we have presented the calculation of the energy-transport velocity in 2D random media, within the low-density approximation of the Bethe-Salpeter equation. Our approach followed closely the derivation of the Amsterdam group,[3] which has been done for a 3D random system. The recently developed[7] coated CPA was extended to a random arrangement of dielectric cylinders. Results for the long-wavelength effective dielectric constant phase velocity, transport velocity, and the localization parameter $k\ell$ are presented for both polarizations.

ACKNOWLEDGMENTS

K.B. acknowledges the financial support of a "DAAD Doktorandenstipendium aus Mitteln des zweiten Hochschulsonderprograms HSPII/AUFE." We want to thank M. Sigalas for useful discussions about his numerical results. Ames Laboratory is operated for the U.S. Department of Energy by Iowa State University under Contract No. W-7405-ENG-82. This work was supported by the Director of Energy Research, Office of Basic Energy Sciences, and NATO Grant No. CRG 940647.

APPENDIX

In this appendix we want to present the scattering coefficients for a coated cylinder consisting of two dielectric materials (inner cylinder dielectric constant ϵ_i, coating material dielectric constant ϵ_c) embedded in a homegenous outer medium with dielectric constant ϵ. Let R_i and R_a be the inner and outer radii of the cylinder, respectively. It is now very convenient to introduce the wave vectors of the different materials by $k_0 = \omega/c$, $k_1 = \sqrt{\epsilon_i}\,k_0$, $k_2 = \sqrt{\epsilon_c}\,k_0$, $k = \sqrt{\epsilon}\,k_0$. Furthermore, we define the size parameters according to $x = kR_i$, $x_1 = k_1R_i$, $x_2 = k_2R_i$, $y = kR_a$, $y_1 = k_1R_a$, and $y_2 = k_2R_a$. Finally, we introduce the following abbreviations: $J_n = J_n(y)$, $J_n^{(2)} = J_n(y_2)$, $H_n = H_n(y)$, and $H_n^{(2)} = H_n(y_2)$. In this notation the van de Hulst scattering coefficients for the coated cylinder can be calculated by standard methods.[18,19] We obtain

$$a_n = \frac{(J_nJ_n^{(2)\prime} - m_2J_n'J_n^{(2)})A_n + (J_nY_n^{(2)\prime} - m_2J_n'Y_n^{(2)})B_n}{(H_nJ_n^{(2)\prime} - m_2H_n'J_n^{(2)})A_n + (H_nY_n^{(2)\prime} - m_2H_n'Y_n^{(2)})B_n},$$

$$b_n = \frac{(m_2J_nJ_n^{(2)\prime} - J_n'J_n^{(2)})C_n + (m_2J_nY_n^{(2)\prime} - J_n'Y_n^{(2)})D_n}{(m_2H_nJ_n^{(2)\prime} - H_n'J_n^{(2)})C_n + (m_2H_nY_n^{(2)\prime} - H_n'Y_n^{(2)})D_n},$$

where the prime denotes the differentiation with respect to the argument and $m_1 = k_1/k$, $m_2 = k_2/k$. Furthermore, we used

$$A_n = \frac{\pi}{2}\,x_1\,[Y_n(x_2)J_n'(x_1) - (k_1/k_2)J_n(x_1)Y_n'(x_2)],$$

$$B_n = \frac{\pi}{2}\,x_1\,[J_n(x_2)J_n'(x_1) - (k_1/k_2)J_n(x_1)J_n'(x_2)],$$

$$C_n = \frac{\pi}{2}\,x_1\,[J_n(x_1)Y_n'(x_2) - (k_1/k_2)Y_n(x_2)J_n'(x_1)],$$

$$D_n = \frac{\pi}{2}\,x_1\,[(k_1/k_2)J_n(x_2)J_n'(x_1) - J_n(x_1)J_n'(x_2)].$$

As usual, J_n, Y_n, and H_n denote the Bessel, von Neumann, and Hankel functions of integer order, respectively.

[1] For a review, see *Scattering and Localization of Classical Waves in Random Media*, edited by Ping Sheng (World Scientific, Singapore, 1990); *Photonic Band Gaps and Localization,* edited by C. M. Soukoulis (Plenum, New York, 1993).
[2] See the special issues of J. Opt. Soc. Am. **10**, 208 (1993) and J. Mod. Opt. **41** (1994).
[3] M. P. van Albada, B. A. van Tiggelen, A. Lagendijk, and A. Tip, Phys. Rev. Lett. **66**, 3132 (1991); Phys. Rev. B **45**, 12 233 (1992); B. A. van Tiggelen and A. Lagendijk, Europhys. Lett. **23**, 311 (1993).
[4] E. Kogan and M. Kaveh, Phys. Rev. B **46**, 10 636 (1992).
[5] G. Cwilich and Y. Yu, Phys. Rev. B **46**, 12 015 (1992).
[6] N. Garcia, A. Z. Genack, and A. A. Lisyansky, Phys. Rev. B **46**, 14 475 (1992); A. A. Lisyansky *et al.*, in *Photonic Band Gaps and Localization* (Ref. 1), p. 171.
[7] C. M. Soukoulis, S. Datta, and E. N. Economou, Phys. Rev. B **49**, 3800 (1994).
[8] K. Busch, C. M. Soukoulis, and E. N. Economou, Phys. Rev. B **50**, 93 (1994).
[9] K. Busch and C. M. Soukoulis (unpublished).
[10] M. Sigalas, C. M. Soukoulis, E. N. Economou, C. T. Chan, and K. M. Ho, Phys. Rev. B **48**, 14 221 (1993).
[11] M. Plihal, A. Shambrook, A. A. Maradudin, and P. Sheng, Opt. Commun. **80**, 199 (1991); M. Plihal and A. A. Maradudin, Phys. Rev. B **44**, 8565 (1991).
[12] R. D. Meade, K. D. Brommer, A. M. Rappe, and J. D. Joannopoulos, Appl. Phys. Lett. **61**, 495 (1992); Phys. Rev. B **44**, 10 961 (1991).
[13] P. R. Villeneuve and M. Piché, Phys. Rev. B **46**, 4969 (1992); **46**, 4973 (1992).
[14] E. N. Economou and M. M. Sigalas, Phys. Rev. B **48**, 13 434 (1993); M. M. Sigalas, E. N. Economou, and M. Kafesaki, *ibid.* **50**, 3393 (1994).
[15] M. M. Sigalas, C. M. Soukoulis, C. T. Chan, and D. Turner (unpublished).
[16] W. M. Robertson, G. Arjavalingam, R. D. Meade, K. D. Brommer, A. M. Rappe, and J. D. Joannopoulos, J. Opt. Soc. Am. B **10**, 322 (1993), and references therein.
[17] D. R. Smith, R. Dalichaonch, N. Kroll, S. Schultz, S. L. McCall, and P. M. Platsman, J. Opt. Soc. Am. B **10**, 314 (1993), and references therein.
[18] H. C. van de Hulst, *Light Scattering of Small Particles* (Dover, New York, 1981).
[19] C. F. Bohren and D. R. Huffman, *Absorption and Scattering of Light by Small Particles* (Wiley, New York, 1983).
[20] Ping Sheng, *Introduction to Wave Scattering, Localization, and Mesoscopic Phenomena* (Academic, New York, 1995).
[21] X. Jing, P. Sheng, and M. Zhou, Phys. Rev. A **46**, 6513 (1992); Physica (Amsterdam) **207A**, 37 (1994).